



HAL
open science

Copper Clusters Containing Hydrides in Trigonal Pyramidal Geometry

Rhone P Brocha Silalahi, Guan-Rong Huang, Jian-Hong Liao, Tzu-Hao Chiu,
Kiran Kumarvarma Chakrahari, Xiaoping Wang, Julien Cartron, Samia
Kahlal, Jean-Yves Saillard, C W Liu

► **To cite this version:**

Rhone P Brocha Silalahi, Guan-Rong Huang, Jian-Hong Liao, Tzu-Hao Chiu, Kiran Kumarvarma Chakrahari, et al.. Copper Clusters Containing Hydrides in Trigonal Pyramidal Geometry. *Inorganic Chemistry*, 2020, 59 (4), pp.2536-2547. 10.1021/acs.inorgchem.9b03501 . hal-02472166

HAL Id: hal-02472166

<https://univ-rennes.hal.science/hal-02472166>

Submitted on 26 Mar 2020

HAL is a multi-disciplinary open access archive for the deposit and dissemination of scientific research documents, whether they are published or not. The documents may come from teaching and research institutions in France or abroad, or from public or private research centers.

L'archive ouverte pluridisciplinaire **HAL**, est destinée au dépôt et à la diffusion de documents scientifiques de niveau recherche, publiés ou non, émanant des établissements d'enseignement et de recherche français ou étrangers, des laboratoires publics ou privés.

Copper Clusters Containing Hydrides in Trigonal Pyramidal Geometry

Rhone P. B. Silalahi,[†] Guan-Rong Huang,[†] Jian-Hong Liao,[†] Tzu-Hao Chiu,[†] Kiran Kumarvarma Chakrahari,[†] Xiaoping Wang,[§] Julien Cartron,[‡] Samia Kahlal,[‡] Jean-Yves Saillard,^{*‡} and C. W. Liu^{*†}

[†]Department of Chemistry, National Dong Hwa University No. 1, Sec. 2, Da Hsueh Rd.

Shoufeng, Hualien 97401 (Taiwan R. O. C.)

[§]Neutron Scattering Division, Neutron Sciences Directorate Oak Ridge National Laboratory, Oak Ridge, TN 37831 (USA)

[‡] Univ Rennes, CNRS, ISCR-UMR 6226, F-35000 Rennes, France

KEYWORDS: Copper, hydride, pentacapped trigonal prism, S-donor ligands

ABSTRACT: Structurally precise copper hydrides $[\text{Cu}_{11}\text{H}_2\{\text{S}_2\text{P}(\text{O}^i\text{Pr})_2\}_6(\text{C}\equiv\text{CR})_3]$, (R= Ph (**1**), $\text{C}_6\text{H}_4\text{F}$ (**2**) and $\text{C}_6\text{H}_4\text{OMe}$ (**3**)) were first synthesized from the polyhydrido copper cluster $[\text{Cu}_{20}\text{H}_{11}\{\text{S}_2\text{P}(\text{O}^i\text{Pr})_2\}_9]$ with nine equiv. of terminal alkynes. Later their isolated yields were significantly improved by direct synthesis from $[\text{Cu}(\text{CH}_3\text{CN})_4](\text{PF}_6)$, $[\text{NH}_4][\text{S}_2\text{P}(\text{O}^i\text{Pr})_2]$, NaBH_4 , and alkynes along with NEt_3 in THF. **1**, **2**, and **3** were fully characterized by single-crystal X-ray diffraction, ESI-MS and multinuclear NMR spectroscopy. All three clusters have eleven copper atoms adopting 3, 3, 4, 4, 4-pentacapped trigonal prismatic geometry, with two hydrides inside the Cu_{11} cage, the position of which being ascertained by a single-crystal neutron diffraction structure of cluster **1** co-crystallized with a $[\text{Cu}_7(\text{H})\{\text{S}_2\text{P}(\text{O}^i\text{Pr})_2\}_6]$, **4** cluster. Six dithiophosphate and three alkynyl ligands stabilize the Cu_{11}H_2 core in which the two hydrides adopt a trigonal pyramidal coordination mode. This coordination mode is so far unprecedented for hydride. The ^1H NMR resonance frequency of the two hydrides appears at 4.8 ppm, a value further confirmed

by ^2H NMR spectroscopy for their deuteride derivatives $[\text{Cu}_{11}(\text{D})_2\{\text{S}_2\text{P}(\text{O}^i\text{Pr})_2\}_6(\text{C}\equiv\text{CR})_3]$. A DFT investigation allows understanding the bonding within this new type of copper(I) hydrides.

INTRODUCTION

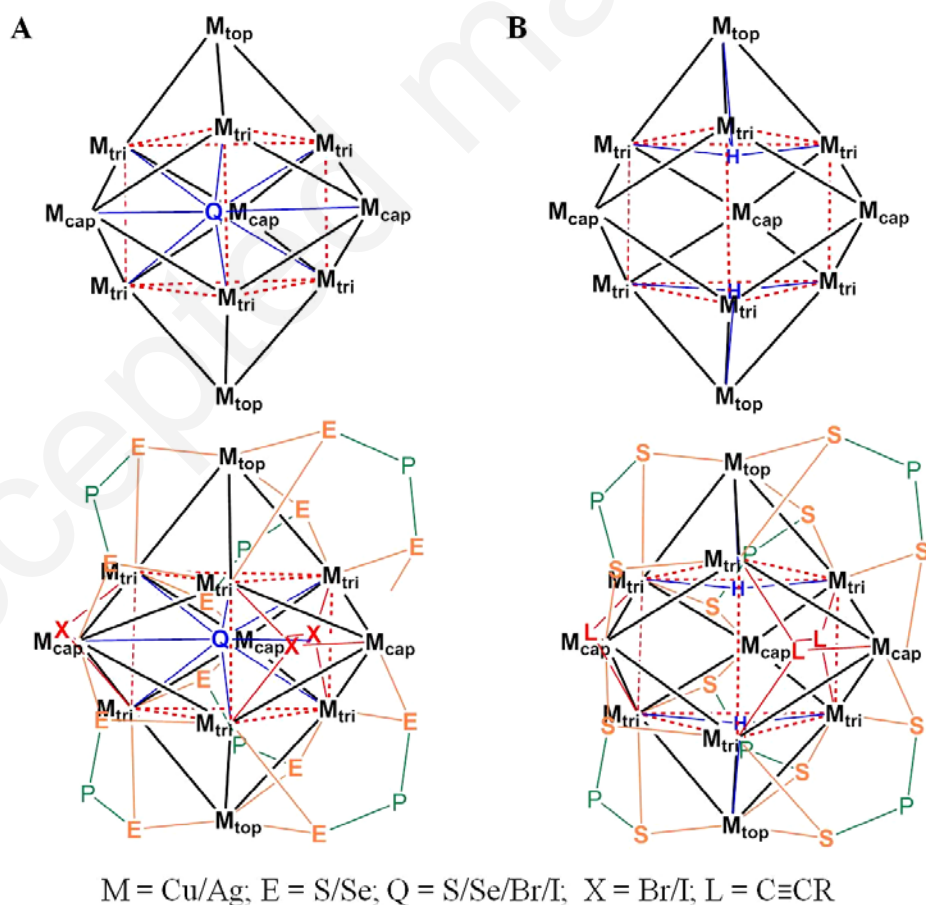
Stereochemistry and properties are strongly related. This is why the exceedingly popular X-ray crystallography technique is the method of choice for understanding molecular properties. However, in the case of hydride-containing complexes and clusters, X-ray diffraction fails to assess the bonding features of the hydride ions, thus not allowing comprehending the properties associated with. This is why rarely has literature addressed the surroundings of hydrides unless neutron diffraction data are available.¹ Under this guideline, our group has managed to uncover new coordination geometry of hydrides from several copper hydrides despite the difficulty in growing good quality single crystals for neutron diffraction.^{1b-f} Among these, five-coordinated hydrides ($\mu_5\text{-H}$) in both square pyramidal and trigonal bipyramidal,^{1b} and four-coordinated hydrides ($\mu_4\text{-H}$) in tetrahedral and square planar^{1f} can be thoroughly discussed. In these compounds, the hypercoordinated hydrides, which are surrounded by a certain number of metal atoms, can be viewed as inverse coordinated centers, within the concept of inversed coordination defined recently by Haiduc,² that is the formation of metal compounds in which the acceptor and donor sites are reversed compared to conventional coordination complexes.

Encapsulation of main group anions in transition metal frameworks remains an active field in cluster science and provides solid examples of inversed coordination. Owing to their variable coordination modes, halides and chalcogenides are the most studied species and have yielded planar, tetrahedral, octahedral, and cubic coordination patterns.² The latter is frequently observed in dithiophosph(in)ate-stabilized M_8^{I} ($\text{M} = \text{Cu}, \text{Ag}$) cubic clusters encapsulating S^{2-} , Cl^- , and Br^- .³ Our research group has reported selenide- and halide-centered cubes, $[\text{Cu}_8(\mu_8\text{-Se})\{\text{Se}_2\text{P}(\text{O}^i\text{Pr})_2\}_6]$,⁴ $[\text{Ag}_8(\mu_8\text{-Se})\{\text{Se}_2\text{P}(\text{O}^i\text{Pr})_2\}_6]$,⁵ $[\text{Cu}_8(\mu_8\text{-X})\{\text{Se}_2\text{P}(\text{OR})_2\}_6](\text{PF}_6)$,⁶ and $[\text{Ag}_8(\mu_8\text{-X})\{\text{Se}_2\text{P}(\text{OR})_2\}_6](\text{PF}_6)$ ($\text{X} = \text{F}, \text{Cl}, \text{Br}$).⁷

The configuration of eleven metal atoms in a pentacapped trigonal prismatic arrangement appears to be prototypical for silver(I) and copper(I) surrounded by both halides and dichalcogenolates. Notable examples are $[\text{Cu}_{11}(\mu_9\text{-Se})(\mu_3\text{-X})_3\{\text{Se}_2\text{P}(\text{OR})_2\}_6]$ ($\text{R} = \text{Et}, \text{Pr}, ^i\text{Pr}$; $\text{X} = \text{Br}, \text{I}$),⁸ $[\text{Ag}_{11}(\mu_9\text{-Se})(\mu_3\text{-X})_3\{\text{Se}_2\text{P}(\text{OR})_2\}_6]$ ($\text{R} = \text{Et}, \text{Pr}, ^i\text{Bu}$; $\text{X} = \text{Br}, \text{I}$)⁹ and $[\text{Ag}_{11}(\mu_9\text{-I})(\mu_3\text{-$

$I_3\{E_2P(O^iPr)_2\}_6$ ($E = S, Se$),¹⁰ $[Cu_{11}(\mu_9-X)(\mu_3-X)_3\{S_2P(O^iPr)_2\}_6]^+$ ($X = Br, I$), and $[Cu_{11}(\mu_9-S)(\mu_3-X)_3\{S_2P(O^iPr)_2\}_6]$ ($X = Br, I$),¹¹ which all house a nanocoordinated sulfide, selenide, or halide at the center of tricapped trigonal-prism (Scheme 1). Cluster stability of this type studied by Density Functional Theory (DFT) has been attributed to the ionocovalent interactions between the central closed-shell anion and the host copper (or silver) atoms, besides the strong M-E (or M-X) covalent bonding. On the other side, encapsulation of two closed-shell anions inside single M_{11} cage is not known, to the best of our knowledge.

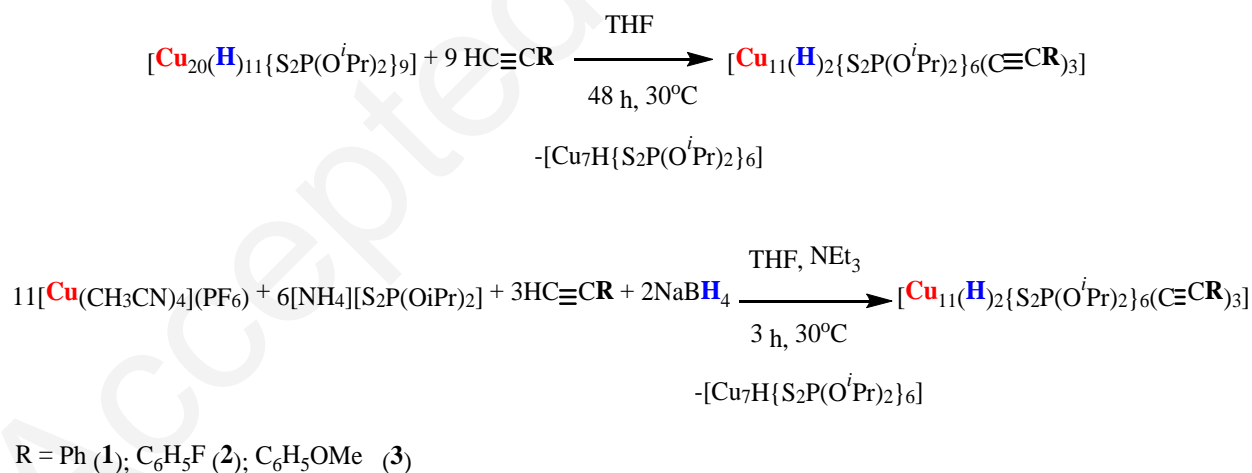
Herein we report three heteroleptic Cu_{11} cages, $[Cu_{11}H_2\{S_2P(O^iPr)_2\}_6(C\equiv CR)_3]$, which contain two encapsulated hydrides. They are produced from the degradation of a polyhydrido copper cluster, $[Cu_{20}H_{11}\{S_2P(O^iPr)_2\}_9]$,^{1e} with nine equiv. of terminal alkynes. Interestingly, this is the first proof of two hydrides located within a pentacapped trigonal prismatic cage of eleven $Cu(I)$ atoms. Unexpectedly, the two hydrides were found to be four-coordinated and exhibiting a brand-new trigonal pyramidal geometry, never observed so far in metal hydride chemistry.



Scheme 1. Sketches of (A) the anion-centered pentacapped trigonal prismatic metal cages stabilized by three halides and six dichalcogenolates; (B) the pentacapped trigonal prismatic copper(I) cage with two interstitial hydrides. The alkoxy groups and phenyl rings are omitted for clarity.

RESULTS AND DISCUSSION

Nine equiv. of terminal alkynes were added to a THF suspension of $[\text{Cu}_{20}\text{H}_{11}\{\text{S}_2\text{P}(\text{O}^i\text{Pr})_2\}_9]$.^{1e} The reaction was stirred at 30°C for 48h and the color of suspension changed from dark orange into dark brown. Workup of this reaction resulted in the isolation of new clusters $[\text{Cu}_{11}(\text{H})_2\{\text{S}_2\text{P}(\text{O}^i\text{Pr})_2\}_6(\text{C}\equiv\text{CR})_3]$, where R= Ph (**1**), C₆H₄F (**2**) and C₆H₄OMe (**3**) as yellow precipitates in 10%, 9.6% and 20.4% yield. The by-products $[\text{Cu}_7(\text{H})\{\text{S}_2\text{P}(\text{O}^i\text{Pr})_2\}_6]$ (**4**) was also formed during the reaction. The yields of **1** and **2** can be increased to 48.7% and 47.4%, respectively, by direct reaction of $[\text{Cu}(\text{CH}_3\text{CN})_4](\text{PF}_6)$, $[\text{NH}_4][\text{S}_2\text{P}(\text{O}^i\text{Pr})_2]$, $[\text{BH}_4]^-$ and alkynes along with NEt₃, where the mole ratios are 3.5:2:1:4:4 at 30°C under N₂ condition (Scheme 2). Their deuteride derivatives $[\text{Cu}_{11}(\text{D})_2\{\text{S}_2\text{P}(\text{O}^i\text{Pr})_2\}_6(\text{C}\equiv\text{CR})_3]$, where R= Ph (**1_D**-50.7%), C₆H₄F (**2_D**-55.3%) and C₆H₄OMe (**3_D**-19.7%) were synthesized to support the existence of hydrides in the cluster.



Scheme 2. General synthesis of **1**, **2** and **3**.

The chemical compositions of **1**, **2**, and **3** were firstly assessed by electrospray ionization mass spectroscopy (ESI-MS) which indicates a band at m/z 2283.54 (calcd. 2283.46) (**1_H**), 2337.49 (calcd. 2337.43) (**2_H**), and 2373.48 (calcd. 2373.49) (**3_H**). ESI-MS also showed a lower-intensity mass peak attributed to the adduct-ion peak of $[\text{Cu}_{11}\text{H}_2\{\text{S}_2\text{P}(\text{O}^i\text{Pr})_2\}_6(\text{C}\equiv\text{CR})_3 + \text{Cu}^+]^+$, at m/z 2346.48 (calcd. 2346.38), 2400.43 (calcd. 2400.36), and 2436.41 (calcd. 2436.42). In addition an adduct ion peak corresponding to $[\text{Cu}_7(\text{H})\{\text{S}_2\text{P}(\text{O}^i\text{Pr})_2\}_6 + \text{Cu}^+]^+$ was also found (Figure S23). The spectra of the deuteride derivatives of **1**, **2** and **3** depict an identical pattern with peaks at m/z 2285.45 (calcd. 2283.46) (**1_D**), 2338.52 (calcd. 2337.43) (**2_D**) and 2375.48 (calcd. 2373.49) (**3_D**). The adduct ions $[\text{X} + \text{Cu}^+]^+$ ($\text{X} = \mathbf{1}, \mathbf{2}$ and $\mathbf{3}$) were also assigned to prominent peaks observed respectively at m/z 2348.37 (calcd 2346.48), 2402.53 (calcd. 2400.36) and 2438.42 (calcd. 2436.42). The simulated isotopic patterns of $[\text{X}]$ and $[\text{X} + \text{Cu}^+]^+$ ($\text{X} = \mathbf{1}, \mathbf{2}$ and $\mathbf{3}$) are in good agreement with the experimental ones as shown in Figures 1 and S17-S22. The peaks of $[\text{X}_\text{H}]$ and $[\text{X}_\text{H} + \text{Cu}^+]^+$ are 1.99 mass unit lower than that of $[\text{X}_\text{D}]$ and $[\text{X}_\text{D} + \text{Cu}^+]^+$, respectively, manifesting the presence of two hydrides in the neutral cluster.

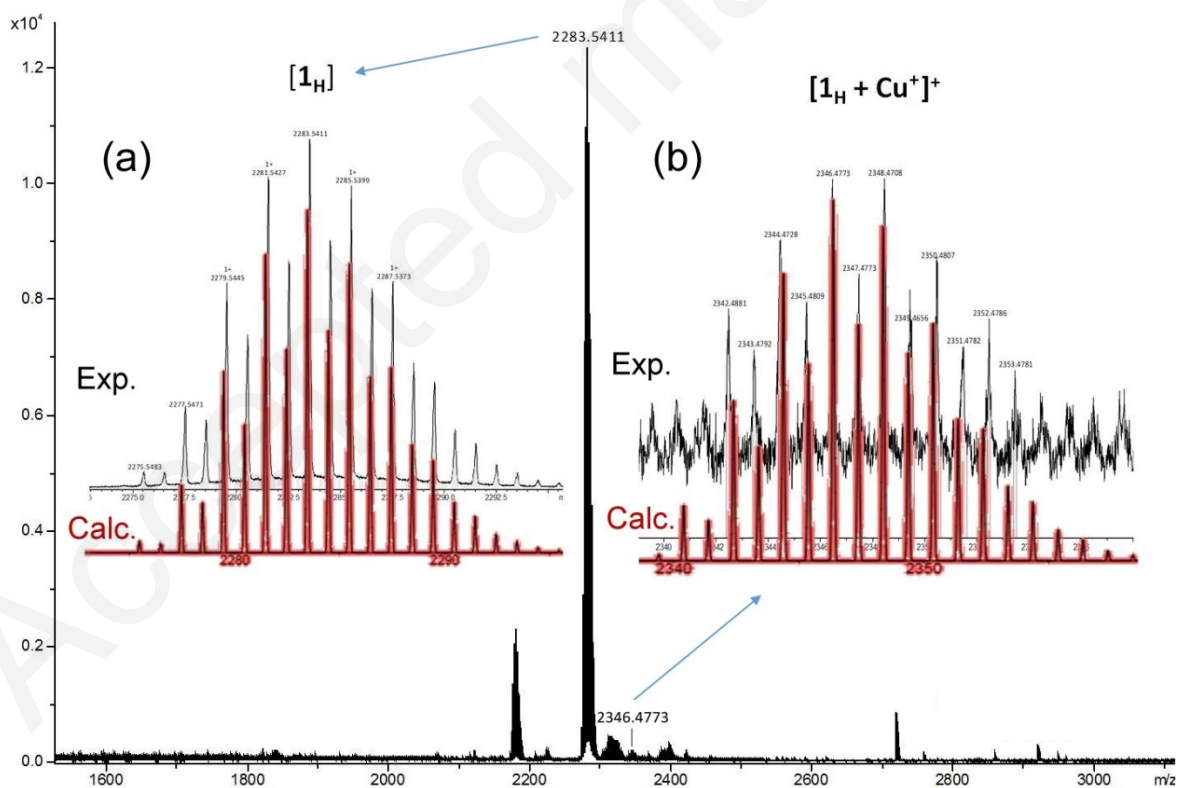


Figure 1. ESI-MS of $[\mathbf{1}_\text{H}]$ and $[\mathbf{1}_\text{H}+\text{Cu}^+]^+$. Inset show experimental and simulated mass spectra of (a) $[\mathbf{1}_\text{H}]$ and (b) $[\mathbf{1}_\text{H}+\text{Cu}^+]^+$.

^1H NMR spectroscopy of clusters **1**, **2**, and **3** displays two sets of proton resonances corresponding to the alkyl group of the dithiophosphate (dtp) ligands and one set of chemical shifts assignable to the alkynyl ligands. However only one ^{31}P chemical shift at 103.9, 103.6 and 104.0 ppm, respectively, is observed for clusters **1** ~ **3** (Figure S6-S11). The observed ^1H NMR chemical shift patterns strongly suggest that there is no two-fold symmetry imposed on the dtp ligand. The two hydrides in **1_H** display a single peak at 4.75 ppm in CDCl_3 (Figure 2a). That of its deuteride analog, **1_D**, appears at 4.82 ppm in chloroform at 297 K (Figure 2b). Comparable values are observed for **2_H** and **2_D** (4.75 and 4.82 ppm, see Figures S1 and S12) and for **3_H** and **3_D** (4.65 and 4.70 ppm, see Figures S2 and S13) in CDCl_3 and CHCl_3 respectively. The accurate integration ratio of ^1H NMR resonances of clusters **1-3** fully confirms their overall compositions, that is: two hydrides, six dithiophosphates and three alkynyl ligands. The FT-IR spectra of the hydride and deuteride derivatives of **1-3** show great similarities. The $\nu(\text{C}\equiv\text{C})$ stretching vibrations of the coordinated alkynyl ligands at 2009.9 (**1_H**), 2001.6 (**2_H**), 2000.9 (**3_H**) and 2010.6 (**1_D**), 2000.4 (**2_D**), 2001.1 (**3_D**) cm^{-1} (Figure S24-S29) are found at lower frequencies than those of the free alkynes ($\nu(\text{HC}\equiv\text{CC}_6\text{H}_5)$)= 2110 cm^{-1} , ($\nu(\text{HC}\equiv\text{C}_6\text{H}_4\text{F})$)= 2115 cm^{-1} and ($\nu(\text{HC}\equiv\text{CC}_6\text{H}_4\text{OCH}_3)$)= 2107 cm^{-1} . These values are slightly lower than that in $[\text{Cu}_{13}\{\text{S}_2\text{CN}^t\text{Bu}_2\}_6(\text{C}_2\text{Ph})_4]^+$ (2019 cm^{-1}).¹²

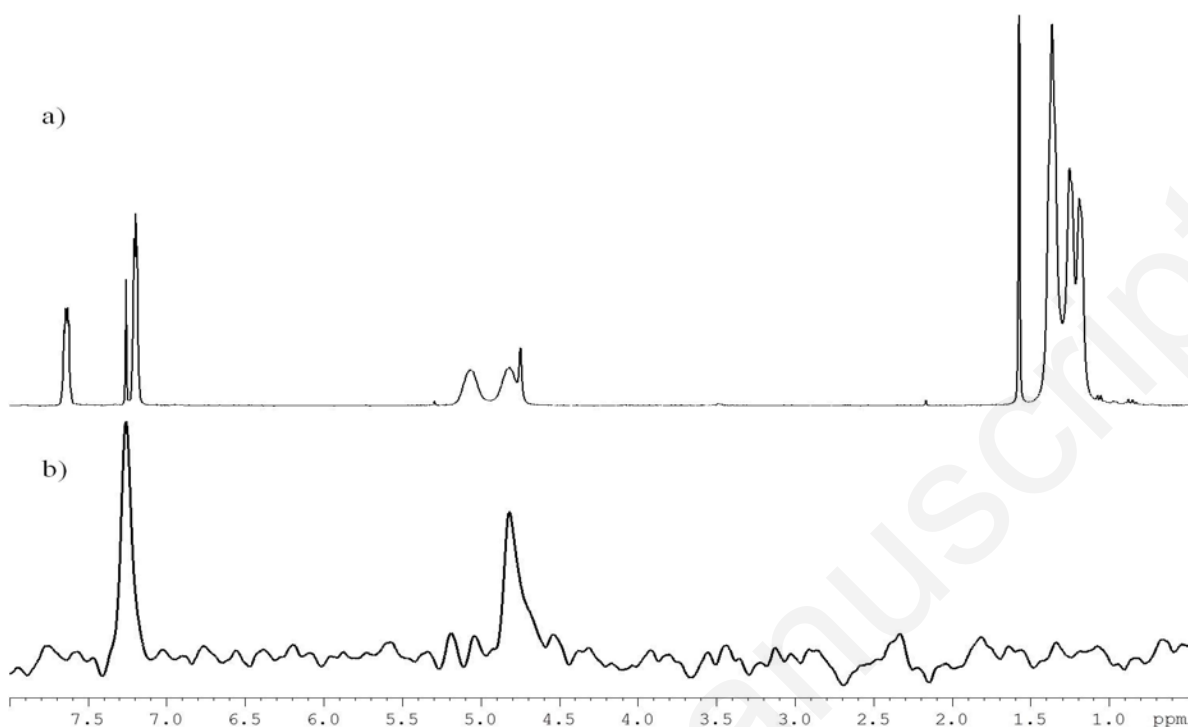


Figure 2. a) ^1H NMR spectrum of compound **1_H** in CDCl_3 and b) ^2H spectrum of compound **1_D** in CHCl_3 .

Selected metric data from the molecular structures of clusters **1-3**, determined by single X-ray and neutron diffraction (vide infra) analyses, are given in Table 1. Views of these molecular structures can be seen in Figure 3 and Figures S31-S33. Their general features are similar and analogous to $[\text{Cu}_{11}(\mu_9\text{-Se})(\text{Br})_3\{\text{S}_2\text{P}(\text{O}^i\text{Pr})_2\}_6]$ and $[\text{Ag}_{11}(\mu_9\text{-I})(\mu_3\text{-I})_3\{\text{E}_2\text{P}(\text{O}^i\text{Pr})_2\}_6]$ [$\text{E}=\text{Se}, \text{S}$].⁸⁻¹¹ The whole copper cage adopts the geometry a 3, 3, 4, 4, 4-pentacapped trigonal prism, *i.e.*, the Cu_6 triangular prism of which the three rectangular and the two triangular faces are capped by an additional copper atom (Figures 3a-3b and S30). The highest ideal symmetry possible for such a Cu_{11} cage is thus D_{3h} . This metal framework is stabilized by three alkynyls and six dtp ligands (Figure 3c). Half of the dtp alkyl groups are oriented towards the alkynes, *i.e.*, along the sides of the metal framework, whereas the remaining half are oriented away from the metal core (Figure 3d). This is in full agreement with the NMR results mentioned above. The six dtp ligands, each bridging four copper atoms in a μ_2, μ_2 binding mode, are equally distributed on the right and left sides of the cluster along the horizontal C_3 axis. The three alkynyl ligands are arranged along the waist of the pentacapped prism, alternatively binding to top and bottom

triangles in $\mu_3\text{-}\eta^1$ fashion. As a result of ligand capping configuration, the ideal D_{3h} symmetry of the Cu_{11} core is lowered to C_{3h} symmetry when the outer ligand sphere is considered. It is of note that, not considering the encapsulated atoms, the structure adopted by **1-3** is similar to that of the above-mentioned clusters $[\text{Cu}_{11}(\mu_9\text{-E})(\mu_3\text{-X})_3\{\text{Se}_2\text{P}(\text{OR})_2\}_6]$ and $[\text{Cu}_{11}(\mu_9\text{-X})(\mu_3\text{-X})_3\{\text{Se}_2\text{P}(\text{OR})_2\}_6]^+$ (E = S, Se; X = halogen),⁹⁻¹¹ with the three $\mu_3\text{-X}$ halides replaced by the three alkynyl ligands. The Cu_6 trigonal prism in **1-3** displays slightly longer intra-triangular edge lengths than the distances of inter-triangular planes. For example, the intra $\text{Cu}_{\text{tri}}\text{-Cu}_{\text{tri}}$ distances are approximately 0.2 Å longer than inter $\text{Cu}_{\text{tri}}\text{-Cu}_{\text{tri}}$ distances (see Table 1). Other distances such as $\text{Cu}_{\text{top}}\text{-Cu}_{\text{tri}}$, $\text{Cu}_{\text{cap}}\text{-Cu}_{\text{tri}}$, and Cu-S are almost identical.

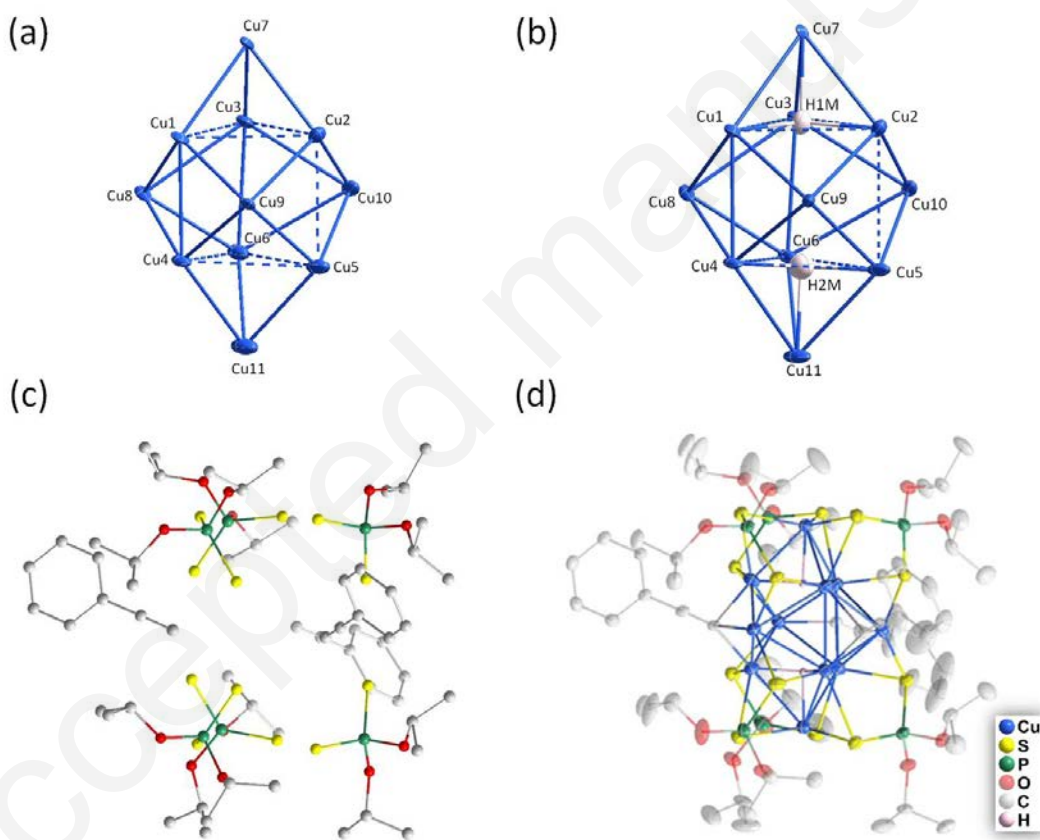


Figure 3. Shell by shell constructions of clusters $[\text{Cu}_{11}(\text{H})_2\{\text{S}_2\text{P}(\text{O}^i\text{Pr})_2\}_6(\text{C}\equiv\text{CR})_3]$, where R= Ph (**1**), $\text{C}_8\text{H}_4\text{F}$ (**2**) and $\text{C}_9\text{H}_7\text{O}$ (**3**) a). A Cu_{11} cage in pentacapped trigonal prism; b) Two hydrides encapsulate the Cu_{11} cage; c) six dithiophosphate and three alkyne ligands; d) Total structure of $[\text{Cu}_{11}(\text{H})_2\{\text{S}_2\text{P}(\text{O}^i\text{Pr})_2\}_6(\text{C}\equiv\text{CR})_3]$.

Comp.	Cu _{tri} -H	Cu _{top} -H	Cu _{tri} -Cu _{tri} intra Cu _{tri} -Cu _{tri} inter	Cu _{top} -Cu _{tri}	Cu _{cap} -Cu _{tri}	Cu-S	Cu-C	C≡C
1	1.69(4)-1.80(4), avg. 1.75(3)	1.82(3)-1.98(4), avg. 1.89(3)	2.9583(6)-3.1667(9), avg. 3.0284(6); 2.7763(5)-2.9245(5), avg. 2.8352(5)	2.5828(5)-2.6274(5), avg. 2.6066(5)	2.5391(5)-2.8400(5), avg. 2.712(5)	2.2801(8)-2.6193(8), avg. 2.3838(8)	1.951(3)-2.131(3), avg. 2.044(3)	1.181(4)-1.220(4), avg. 1.206(4)
1_N	1.737(19)-1.793(17), avg. 1.76(2)	1.841(19), 1.860(17) avg. 1.851(18)	2.989(11)-3.17(1), avg. 3.05(1) 2.771(8)-2.902(9), avg. 2.842(8)	2.556(9)-2.659(11), avg. 2.601(10)	2.509(8)-2.892(9), avg. 2.718(10)	2.24(2)-2.618(16), avg. 2.38(2)	1.951(11)-2.158(9), avg. 2.043(10)	1.201 (11)- 1.204(10) avg. 1.203(11)
1' (DFT)	1.714-1.784, avg. 1.749	1.880-1.896, avg. 1.888	2.854-3.221, avg. 3.024 2.903-2.958, avg. 2.932	2.566-2.609, avg. 2.584	2.531-3.087, avg. 2.773	2.290-2.709, avg. 2.402	1.944-2.160, avg. 2.044	1.237-1.238 avg. 1.238
2	1.66(5)-1.87(5), avg. 1.77(5)	1.78(4)-1.89(5), avg. 1.85(5)	2.9644(7)-3.195(1), avg. 3.049(1) 2.7550(6)-2.9370(6), avg. 2.8631(6)	2.5464(6)-2.6417(6), avg. 2.6098(6)	2.5425(6) – 3.0179(6), avg. 2.7439(6)	2.2784(9)-2.7153(11), avg. 2.3858(9)	1.930(4)-2.157(4), avg. 2.044(3)	1.185(5)-1.223(5), avg. 1.209(5)
3	1.72(4)-1.80(4), avg. 1.76(4)	1.88(4)- 2.04(4), avg. 1.96(4)	2.9953(5)-3.1004(6), avg. 3.0468(6); 2.7366(4)-2.8527(5), avg. 2.7808(4)	2.6021(4)-2.6244(4), avg. 2.6154(4)	2.5762(4)-2.8344(4), avg. 2.7125(4)	2.3002(6)-2.5896(7), avg. 2.3902(7)	1.950(3)-2.125(3), avg. 2.046(2)	1.214(4)-1.218(4), avg. 1.216(4)
3 (DFT)	1.732-1.744, avg. 1.738	1.896-1.905, avg. 1.901	2.952-3.069, avg. 3.009 2.755-2.814 avg. 2.776	2.580-2.622, avg. 2.601	2.568-2.793, avg. 2.697	2.310-2.529, avg. 2.389	1.956-2.139, avg. 2.044	1.230-1.232, avg. 1.231

Table 1. Selected bond lengths (Å) for **1**, **2**, and **3** (X-ray data), **1_N** (neutron data), **1'** and **3** (DFT).

Table 2. Selected crystallographic data of **1-3** (X-ray) and **2[1_N] · [4_N]** (neutron).

	1	2	3 · 2(C ₆ H ₁₄) · [(CH ₃) ₂ CO]	2[1 _N] · [4 _N] · 2[(CH ₃) ₂ CO]
CCDC number	1961353	1961354	1961355	1967640
Empirical formula	C ₆₀ H ₁₀₁ Cu ₁₁ O ₁₂ P ₆ S ₁₂	C ₃₆₃ H _{593.20} Cu ₆₆ F ₁₈ O ₇₃ P ₃₆ S _{72.4}	C ₇₈ H ₁₄₁ Cu ₁₁ O ₁₆ P ₆ S ₁₂	C ₁₆₄ H ₃₀₀ Cu ₂₉ O ₃₈ P ₁₈ S ₃₆
Formula weight	2283.88	14097.24	2604.38	6434.30
Temperature, K	150(2)	150(2)	150(2)	100(2)
Wavelength, Å	0.71073	0.71073	0.71073	0.4 - 3.5
Crystal system	Triclinic	Monoclinic	Triclinic	Triclinic
Space group	<i>P</i> (-) <i>1</i>	<i>P</i> 2 ₁ / <i>n</i>	<i>P</i> (-) <i>1</i>	<i>P</i> (-) <i>1</i>
<i>a</i> , Å	14.9244(14)	23.7795(10)	14.9538(6)	14.5541(5)
<i>b</i> , Å	26.487(3)	27.3755(12)	15.0769(6)	19.9817(7)
<i>c</i> , Å	28.342(3)	41.2995(18)	27.7010(10)	23.5820(8)
α , deg.	113.149(2)	90	82.7840(10)	105.344(3)
β , deg.	104.257(2)	90.1670(10)	86.5970(10)	102.635(3)
γ , deg.	97.301(2)	90	61.0810(10)	98.626(3)
Volume, Å ³	9664.2(16)	26885(2)	5423.3(4)	6294.0(4)
<i>Z</i>	4	2	2	1
Calculated density, Mg m ⁻³	1.570	1.741	1.595	1.698
Absorption coefficient, mm ⁻¹ (neutron, cm ⁻¹)	2.772	2.998	2.483	1.1587 + 0.8921 λ
Crystal size, mm ³	0.07 x 0.08 x 0.15	0.13 x 0.23 x 0.33	0.29 x 0.36 x 0.38	0.80 x 1.24 x 1.75
θ_{\max} , deg.	25.000	26.399	27.136	32.625
Reflections collected / unique	86957 / 33948 (<i>R</i> _{int} = 0.0211)	234576 / 55078 (<i>R</i> _{int} = 0.0427)	77464 / 23970 (<i>R</i> _{int} = 0.0229)	20644 / 10153 (<i>R</i> _{int} = 0.1249)
Completeness, %	99.7	100.0	100.0	38.8
restraints / parameters	947 / 1893	1320 / 3026	522 / 1147	4707 / 2513
GoF	1.068	1.024	1.064	1.127
Final <i>R</i> indices [<i>I</i> > 2 σ (<i>I</i>)]	<i>R</i> 1 = 0.0268, <i>wR</i> 2 = 0.0678	<i>R</i> 1 = 0.0346, <i>wR</i> 2 = 0.0747	<i>R</i> 1 = 0.0307, <i>wR</i> 2 = 0.0745	<i>R</i> 1 = 0.1425, <i>wR</i> 2 = 0.2718
<i>R</i> indices (all data)	<i>R</i> 1 = 0.0341, <i>wR</i> 2 = 0.0703	<i>R</i> 1 = 0.0522, <i>wR</i> 2 = 0.0810	<i>R</i> 1 = 0.0343, <i>wR</i> 2 = 0.0762	<i>R</i> 1 = 0.1427, <i>wR</i> 2 = 0.2722
Largest diff. peak / hole, e Å ⁻³ (neutron, fm)	1.389, -0.797	3.568, -2.465	2.345, -0.910	1.235, -0.903

The precise hydride positions were ascertained by a single-crystal neutron diffraction study of a co-crystallized compound labeled $2[\mathbf{1}_N] \cdot [\mathbf{4}_N] \cdot 2[(\text{CH}_3)_2\text{CO}]$, which contains two clusters $[\text{Cu}_{11}(\text{H})_2\{\text{S}_2\text{P}(\text{O}^i\text{Pr})_2\}_6(\text{C}\equiv\text{CPh})_3]$ (**1**), one $[\text{Cu}_7(\text{H})\{\text{S}_2\text{P}(\text{O}^i\text{Pr})_2\}_6]$ (**4**), and two acetone molecules in the asymmetric unit. The hydride atoms were located in the nuclear density map and refined anisotropically. The OMIT map in Figure 4a shows the distribution of negative nuclear densities of the two hydrides. They occupy symmetrical positions in each of the (top and bottom) metal tetrahedral cavity composed of a prismatic triangular face and its capping atom. Surprisingly, they do not sit at the tetrahedron center, but instead are lying almost in the plane of the triangular face, as indicated by the sum of the $\text{Cu}_{\text{tri}}\text{-H-Cu}_{\text{tri}}$ angles, which is close to 360 degree (Figure 4). As far as we know, this trigonal pyramidal coordination mode of hydrides characterized by neutron diffraction is unprecedented. Indeed the coordination environment of a four-coordinate hydride is mostly in tetrahedral or near square-planar geometry.¹ The Cu-H distances reflect the trigonal pyramidal coordination with two types of Cu-H distances, $\text{Cu}_{\text{tri}}\text{-H}$ (average 1.76(2) Å) and $\text{Cu}_{\text{top}}\text{-H}$ (average 1.851(18) Å). Selected bond lengths of **1**_N are listed in Table 1. The ³¹P NMR resonances of the co-crystals are at 104.16 ppm (**1**) and 103.95 ppm (**4**) in a 2:1 ratio (Figure S35). The overall composition of $[2(\mathbf{1})(\mathbf{4})]$ was further characterized by ESI-mass spectrometry (Figure S36).

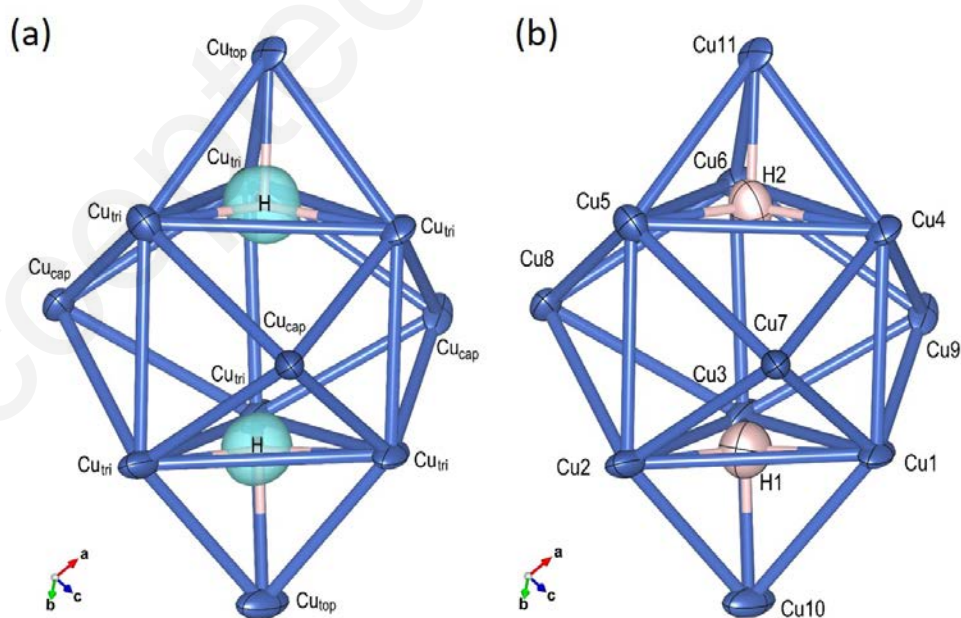


Figure 4. (a) Overlay of the omit map showing the negative nuclear scattering density of the missing hydride atoms in the Cu_{11}H_2 core of **1_N** (neutron data). (b) View of the hydride atoms in the Cu_{11}H_2 core of **1_N** showing the atom labeling scheme. Atomic displacement ellipsoids are drawn at their 50% probability level. Color code: Cu, blue; H, pink; nuclear density, cyan. The nuclear density is displayed at isosurface level of $-1.0 \text{ fm } \text{\AA}^{-3}$. Selected geometric parameters (\AA ; $^\circ$): H1–Cu1 1.751(19), H1–Cu2 1.78(2), H1–Cu3 1.77(2), H1–Cu10 1.841(19); H2–Cu4 1.793(17), H2–Cu5 1.741(17), H2–Cu6 1.737(19), H2–Cu11 1.860(17); Cu1–H1–Cu3 116.5(12), Cu1–H1–Cu2 117.0(13), Cu3–H1–Cu2 126.1(11), Cu1–H1–Cu10 90.7(9), Cu3–H1–Cu10 94.9(11), Cu2–H1–Cu10 90.8(9), Cu6–H2–Cu5 118.5(9), Cu6–H2–Cu4 122.7(9), Cu5–H2–Cu4 118.4(10), Cu6–H2–Cu11 92.7(8), Cu5–H2–Cu11 91.0(8), Cu4–H2–Cu11 92.2(8). Displacement of hydride atoms from the plane defined by each of the three Cu_{tri} atoms: - 0.068(19) \AA for H1 and 0.061(16) \AA for H2.

The $[\text{Cu}_{11}(\text{H})_2\{\text{S}_2\text{P}(\text{O}^i\text{Pr})_2\}_6(\text{C}\equiv\text{CR})_3]$ clusters look yellowish to the naked eye and have similar absorption features. Clusters **1**, **2** and **3** display two intense prominent absorption bands at 344 and 414 nm for **1**, 343 and 414 nm for **2** and 344 and 411 nm for **3** (Figure 5). The compound **[(1)₂(4)]** containing the co-crystallized **1** and **4** clusters in the solid state is also yellowish and its spectrum shows the distinguished absorption of both components (Figure S37), *i.e.*, two absorption bands characteristic of **4** at 286 nm and 348 nm and a broad absorption band around 418 nm for **1**. Monitoring the stability of **1** in dichloromethane by UV-Vis at ambient temperature indicates it changes steadily over time and completely decomposes within 5 days (Figure S38). Furthermore, the variable temperature ^1H NMR spectra show that resonances corresponding to the alkyl groups of dtp and phenylacetylene moieties remain unchanged and the two hydrides peaks at 4.86 ppm still exist during heating process (Figure S39). This result indicates that **1** is stable at elevated temperature.

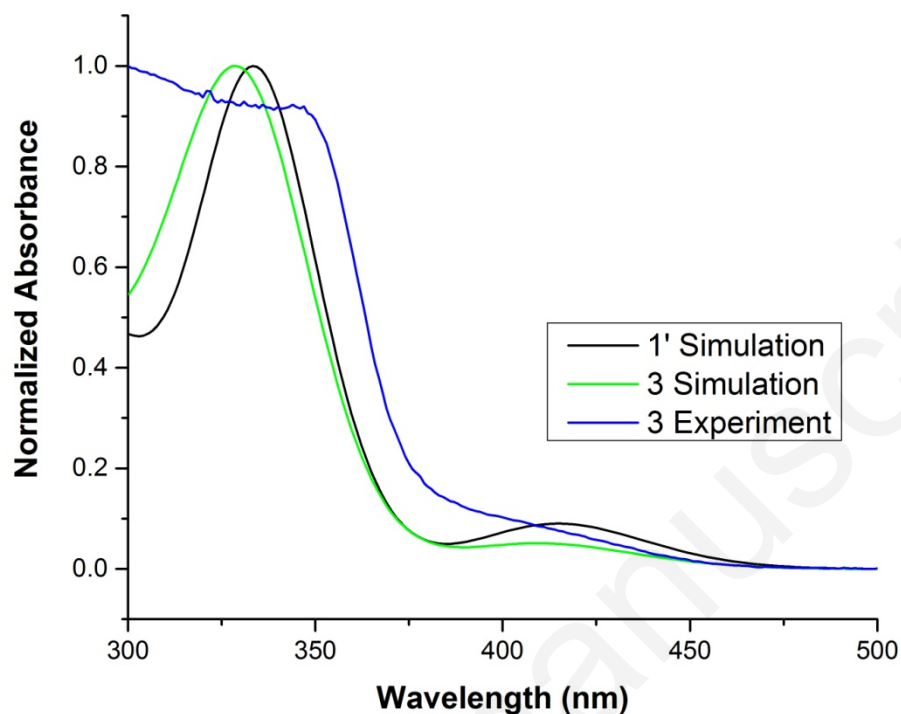


Figure 5. The absorption spectra of cluster **3** in dichloromethane (1.07×10^{-5} M) and calculated spectra of **1'** and **3**.

DFT calculations carried out at the PBE0/Def2TZVP level were performed both on a simplified model of compounds **1-3**, namely $[\text{Cu}_{11}(\text{H})_2(\text{S}_2\text{PH}_2)_6(\text{C}_2\text{Ph})_3]$ (**1'**) and on the cluster **3**. Their optimized geometries were found to be of C_i symmetry, the deviation away from ideal C_{3h} symmetry being mainly due to space filling of the ligand substituents. Their metric data are fully consistent with their experimental counterparts in clusters **1-3** (Table 1). It is noteworthy that the trigonal pyramidal coordination mode of the hydrides found by neutron diffraction is unambiguously reproduced by DFT. Other hydride positions were tested in the case **1'**. Any trial to encapsulate them in other cavities ended up with the optimized geometry of the global energy minimum, *i.e.* encapsulated hydrides along the pseudo- C_3 axis in trigonal pyramidal coordination, presumably in part because of the larger size of these alternative 5-atom cavities, but overall for orbital matching requirement (see below). Similar results were obtained when looking for hydride outer capping positions. A unique alternative energy minimum was found with the hydrides bonded in terminal positions to the Cu_{top} atoms lying on the C_3 axis. This high-

energy isomer was found to lie 4.48 eV above the global minimum and thus has virtually no chance to be observed. The large HOMO-LUMO gaps of **1'** and **3** (3.72 and 3.70 eV, respectively) are typical for stable Cu(I) hydride nanoclusters.^{1b-f}

Table 3. Selected NAO charges and interatomic Wiberg indices computed for **1'**.

NAO charges	Cu _{tri}	0.74
	Cu _{top}	0.68
	Cu _{cap}	0.74
	H (hydrides)	-0.69
Wiberg indices	Cu _{tri} -H	0.097
	Cu _{top} -H	0.070
	Cu _{tri} -Cu _{tri}	0.025
	Cu _{top} -Cu _{tri}	0.040
	Cu _{cap} -Cu _{tri}	0.032
	Cu – S	0.157
	Cu – C	0.178
	C≡C	2.624

Since **1'** and **3** provided very similar results, we focus below on those of **1'**. Its Kohn-Sham orbital diagram is shown in Figure 6. The highest occupied levels have a dominant 3d(Cu) character with negligible hydride participation. The three lowest unoccupied orbitals are the combination of “in-plane” $\pi^*(CC)$ orbitals of the phenyl alkynyl ligands. They are delocalized on both the CC triple bonds and the 6-membered rings with minor metal admixtures. The natural atomic orbital (NAO) charges of the copper atoms ($\sim +0.7$, see Table 3) and of the hydrides (~ -0.7) are also typical for stable Cu(I) hydride nanoclusters.^{1b-f} The particularly small Cu-Cu Wiberg indices are consistent with the mainly metallophilic character of these weak interactions. The Cu-H Wiberg indices indicate stronger bonding with the in-plane Cu_{tri} atoms, in line with their shorter Cu-H distances (Table 1).

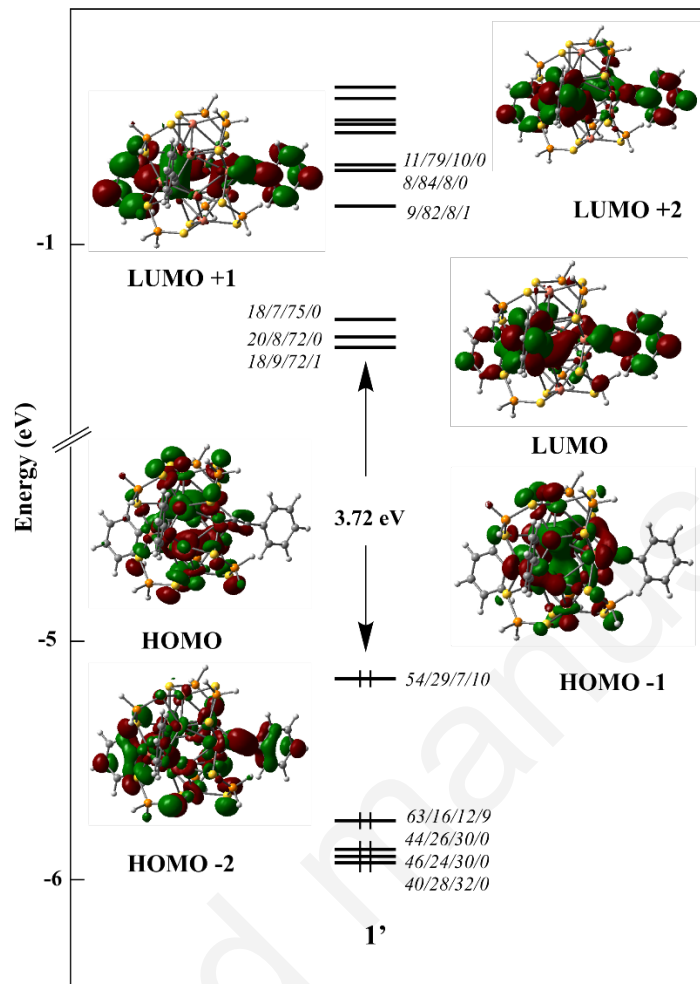


Figure 6. Kohn-Sham frontier orbital diagram of cluster **1'** with localization (%) in the order $\text{Cu}_{11}/(\text{S}_2\text{PH}_2)_6/(\text{C}_2\text{Ph})_3/\text{H}_2$.

An analysis of the bonding of the two hydrides with their $[\text{Cu}_{11}(\text{S}_2\text{PH}_2)_6(\text{C}_2\text{Ph})_3]^{2+}$ host cage in **1'** leads to a very simple 2-electron/2-orbital picture: both in-phase and out-of-phase combinations of the occupied $1s(\text{H})$ orbitals interact in a one-to-one fashion with the LUMO and LUMO+1 of $[\text{Cu}_{11}(\text{S}_2\text{PH}_2)_6(\text{C}_2\text{Ph})_3]^{2+}$, respectively. These two accepting orbitals (Figure 7) have large $4s(\text{Cu})$ character, both with major localization on the triangular faces of the central copper prisms (49 % and 51%, respectively) and minor contribution (9% and 13%, respectively) on the copper atoms capping these faces. These orbital topologies are responsible for the preference for a nearly trigonal pyramidal hydride coordination mode over the more common tetrahedral one. The larger $\text{Cu}\dots\text{Cu}$ distances of the trigonal base ($\text{Cu}_{\text{tri}}\text{-Cu}_{\text{tri}}$ intra in Table 1) also favor this preference.

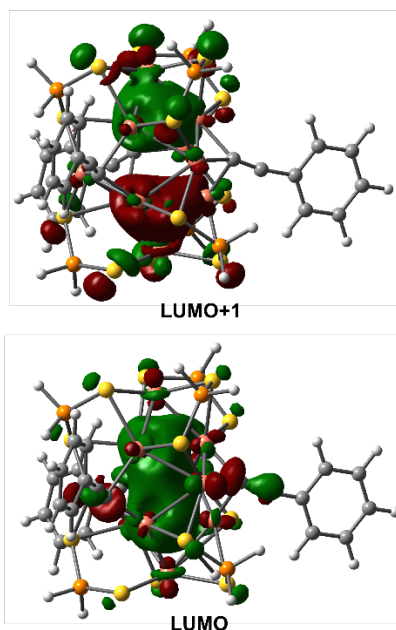


Figure 7. The two accepting orbitals of the hosting cage $[\text{Cu}_{11}(\text{S}_2\text{PH}_2)_6(\text{C}_2\text{Ph})_3]^{2+}$ which are responsible for the bonding with the two encapsulated hydrides.

TD-DFT calculations on **1'** found the simulated low-energy weak band (Figure 5) associated with a transition at 415 nm of HOMO \rightarrow LUMO and HOMO \rightarrow LUMO+1 character, thus of MLCT nature, where L means mainly alkynyl $\pi^*(\text{CC})$. The second simulated band is associated with a transition at 333 nm also of MLCT nature, and involves several 3d(Cu)-type occupied levels and the three lowest vacant orbitals of large alkynyl $\pi^*(\text{CC})$ nature. The TD-DFT-simulated spectrum of **3** (Figure 5) is very similar to that of **1'**, with transitions of the same MLCT nature.

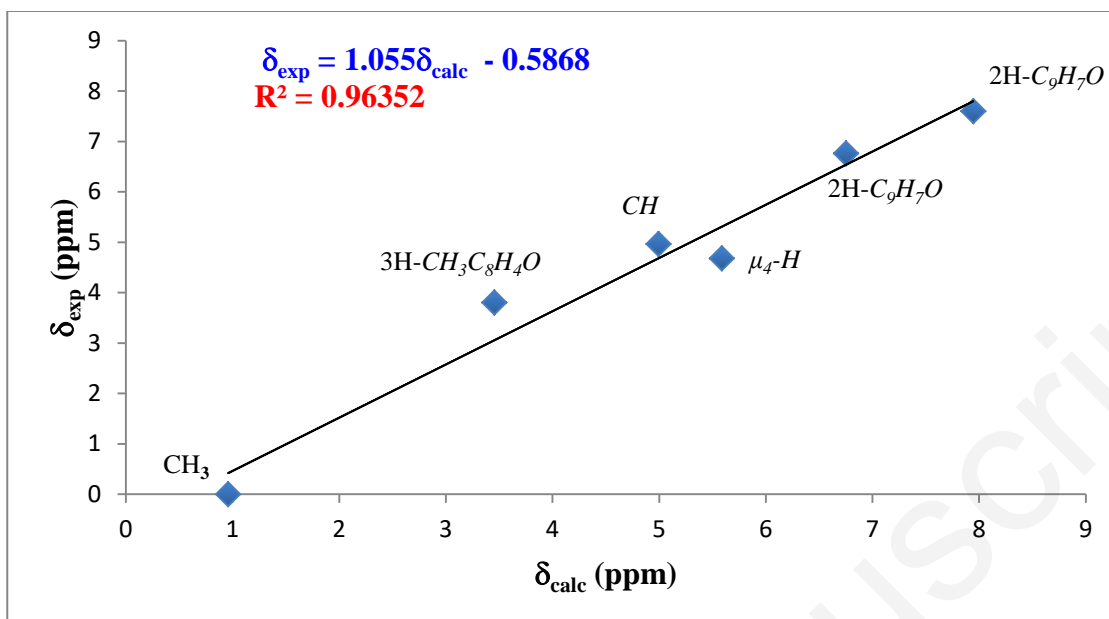


Figure 8. A correlation plot of the experimental vs. computed ^1H NMR chemical shifts of **3**.

Finally, it is worthy of noting that the calculated ^1H NMR chemical shifts of **3** are in good agreement with their experimental counterparts, as exemplified by the linear correlation that exists between the two sets of values (Figure 8). Such a consistency brings supplementary confidence on the existence of the two encapsulated hydrides and on their coordination mode, if there were even the need for. Finally, it should be noted that the calculated Cu-H vibrational frequencies were found to lie in two ranges, *i.e.* $730\text{-}790\text{ cm}^{-1}$ and $1200\text{-}1220\text{ cm}^{-1}$.

CONCLUSIONS

We have successfully isolated three new clusters, $[\text{Cu}_{11}(\text{H})_2\{\text{S}_2\text{P}(\text{O}^i\text{Pr})_2\}_6(\text{C}\equiv\text{CR})_3]$, R= Ph (**1**), $\text{C}_6\text{H}_4\text{F}$ (**2**) and $\text{C}_6\text{H}_4\text{OMe}$ (**3**), which contain two hydrides located inside an eleven-copper cage. The Cu_{11}H_2 core is the first example having two interstitial hydrides enclosed in a pentacapped trigonal prismatic copper cage, which is further stabilized by six diisopropyl dithiophosphates and three alkynyl ligands. The two hydrides in **1** adopt a μ_4 -H trigonal pyramidal coordination mode, fully authenticated by single crystal neutron diffraction and confirmed by DFT calculations. The fully characterized copper hydrides provide timely examples for the emerging topics of

nanoscale copper hydrides,^{14a-g} the hydride position of some of which being not even discussed.^{14h-j}

EXPERIMENTAL SECTIONS

All chemicals were purchased from commercial sources and used as received. Solvents were purified following standard protocols. All reactions were carried out under N₂ atmosphere by using standard Schlenk techniques. [Cu₂₀H₁₁{S₂P(O^{*i*}Pr)₂}₉],^{1e} [Cu(CH₃CN)₄](PF₆)₂,¹⁵ and [NH₄][S₂P(O^{*i*}Pr)₂]₆¹⁶ was prepared by following the procedure reported in literature and characterized.¹⁶ NMR spectra were recorded on a Bruker Advance DPX300 FT-NMR spectrometer operating at 300 MHz while recording ¹H, 121.5 MHz for ³¹P, 100.61 MHz for ¹³C and 46.1 MHz for ²H. The ³¹P NMR spectra were referenced to external 85% H₃PO₄ at δ=0 ppm. The chemical shift (δ) and coupling constant (J) are reported in ppm and Hz, respectively. ESI-mass spectrum recorded on a Fison Quattro Bio-Q (Fisons Instruments, VG Biotech, U. K.). UV-Visible absorption spectra were measured on a Perkin Elmer Lambda 750 spectrophotometer using quartz cells with a path length of 1 cm.

General Preparation of [Cu₁₁(H)₂{S₂P(O^{*i*}Pr)₂}₆(C≡CR)₃], [R= C₂Ph (1); C₈H₄F (2); C₉H₇O (3)]. Cluster 1, 2, and 3 can be prepared by following two general procedures and detailed preparation method is given for cluster 1 for both methods.

Method a (1-3). In a Flame-dried Schlenk tube, [Cu₂₀(H)₁₁{S₂P(O^{*i*}Pr)₂}₉], (0.1 g, 0.031 mmol) was suspended in THF (5 cm³) along with phenylacetylene (31 μL, 0.279 mmol) resulting mixture was stirred at 30 °C for 48 h. The solvent was evaporated under vacuum and residue was dissolved in DCM and washed with water (3×15mL). After separation, organic layer was passed through Al₂O₃, the yellow residue was dissolved with ether, and solvent was evaporated under vacuum. The precipitate continue to wash with methanol (3x15 mL), to remove [Cu₇H{S₂P(O^{*i*}Pr)₂]₆] and ligands impurities. Finally, solvent was evaporated to dryness under vacuum to get a pure yellow powdered of **1**. The yield is 0.0655, 10.1% based on Cu.

Similarly, deuterium analog (**3**) was synthesized by using [Cu₂₀(D)₁₁{S₂P(O^{*i*}Pr)₂}₉], result the formation of [Cu₁₁(D)₂{S₂P(O^{*i*}Pr)₂}₆(C≡CC₄H₉OMe)₃].

Method b (1-2). In a Flame-dried Schlenk tube $[\text{NH}_4][\text{S}_2\text{P}(\text{O}^i\text{Pr})_2]$ (0.046 g, 0.2 mmol) and phenylacetylene (43 μL , 0.4 mmol) was suspended in THF (30 cm^3), then continue addition of $[\text{Cu}(\text{CH}_3\text{CN})_4](\text{PF}_6)$ (0.112 g, 0.35 mmol) and Triethylamine (40 μL , 0.4 mmol). After stirred 5 minute, NaBH_4 (0.0037 g, 0.1 mmol) was added to the mixture. The resulting mixture was stirred at 30°C for 3 hours. The solvent was evaporated under vacuum and residue was dissolved in DCM and washed with water (3 \times 15mL). After separation, organic layer was passed through Al_2O_3 , the yellow residue was dissolved with ether, and solvent was evaporated under vacuum. The precipitate continue to wash with methanol (3x15 mL), to remove $[\text{Cu}_7\text{H}\{\text{S}_2\text{P}(\text{O}^i\text{Pr})_2\}_6]$ and ligands impurities. Finally, solvent was evaporated to dryness under vacuum to get a pure yellow powdered of **1**. The yield is 0.030, 48.7% based on Cu.

Similarly, deuterium analog (**1-2**) was synthesized by reacting NaBD_4 (0.0042, 0.1 mmol), result the formation of $[\text{Cu}_{11}(\text{D})_2\{\text{S}_2\text{P}(\text{O}^i\text{Pr})_2\}_6(\text{C}\equiv\text{CR})_3]$.

Preparation of 2[1] . [4]

In a Flame-dried Schlenk tube $[\text{NH}_4][\text{S}_2\text{P}(\text{O}^i\text{Pr})_2]$ (0.046 g, 0.2 mmol) and phenylacetylene (43 μL , 0.4 mmol) was suspended in THF (30 cm^3), then continue addition of $[\text{Cu}(\text{CH}_3\text{CN})_4](\text{PF}_6)$ (0.112g, 0.35 mmol) and Triethylamine (40 μL , 0.4 mmol). After stirred 5 minute, NaBH_4 (0.0037 g, 0.1 mmol) was added to the mixture. The resulting mixture was stirred at 30°C for 3 hours. The solvent was evaporated under vacuum and residue was dissolved in DCM and washed with water (3 \times 15mL). After extraction, organic layer was collected and passed through Al_2O_3 to get yellow residue then dissolved in acetone. Solvent was evaporated under vacuum to get yellow powders of **1** and **4**.

(1_H): ESI-MS: m/z (Cal. 2283.46) 2283.54 for $[\text{Cu}_{11}(\text{H})_2\{\text{S}_2\text{P}(\text{O}^i\text{Pr})_2\}_6(\text{C}\equiv\text{CC}_6\text{H}_5)_3]$ (**1_H**) and m/z (Cal. 2346.38) 2346.48 for $[\text{Cu}_{11}(\text{H})_2\{\text{S}_2\text{P}(\text{O}^i\text{Pr})_2\}_6(\text{C}\equiv\text{CC}_6\text{H}_5)_3]+\text{Cu}^+$. ^1H NMR (300 MHz, CDCl_3): 7.21~7.65 (m, 15 H, $-\text{C}_2\text{Ph}$), 5.07~4.83 (m, 12 H, CH), 4.76 (bs, 2H, $\mu_4\text{-H}$), 1.52~1.38 (d, 72 H, CH_3) ppm; ^{13}C NMR (400 MHz, d -Acetone): 135.25, 131.75, 128.12, 124.13, 83.87, 74.58, 74.07, 73.12, 23.31 ppm; ^{31}P NMR (121.49 MHz, CDCl_3): 103.9 (**1_H**). FT-IR data in KBr pellet (cm^{-1}): 2975.3; 2931.9; 2870.7; 2009.9; 1722.7; 1592.5; 1483.3; 1177.1; 1140.2 1069.1; 951.7, 884.1; 755.8; 689.6. Elem.Anal: (Cal. C% 31.55; H% 4.46). Found: C% 31.21; H% 4.50.

(1_D): ESI-MS: m/z (Cal. 2283.46) 2285.45 for $[\text{Cu}_{11}(\text{D})_2\{\text{S}_2\text{P}(\text{O}^i\text{Pr})_2\}_6(\text{C}\equiv\text{CC}_6\text{H}_5)_3]$ (**1_D**) and m/z (Cal. 2346.38) 2348.37 for $[\text{Cu}_{11}(\text{D})_2\{\text{S}_2\text{P}(\text{O}^i\text{Pr})_2\}_6(\text{C}\equiv\text{CC}_6\text{H}_5)_3]+\text{Cu}^+]^+$. ^1H NMR (300 MHz, CDCl_3): 7.20~7.65 (m, 15 H, $-\text{C}_2\text{Ph}$), 5.07~4.82 (m, 12 H, CH), 1.52~1.38 (d, 72 H, CH_3) ppm. ^2H NMR (46.1 MHz, CDCl_3): 4.82 (bs, 2D, $\mu_4\text{-D}$). ^{31}P NMR (121.49 MHz, CDCl_3): 103.9 (**1_H**). FT-IR data in KBr pellet (cm^{-1}): 2976.1; 2932.1; 2871.6; 2010.6, 1723.6; 1592.7; 1482.9; 1177.1; 1064.4; m951.6; 884.4; 753.7; 689.7. The percentage yield: 0.032 g, 50.7% based on Cu.

(2_H): ESI-MS: m/z (Cal. 2337.43) 2337.49 for $[\text{Cu}_{11}(\text{H})_2\{\text{S}_2\text{P}(\text{O}^i\text{Pr})_2\}_6(\text{C}\equiv\text{CC}_6\text{H}_5\text{F})_3]$ (**2_H**) and m/z (Cal. 2400.36) 2400.43 for $[\text{Cu}_{11}(\text{H})_2\{\text{S}_2\text{P}(\text{O}^i\text{Pr})_2\}_6(\text{C}\equiv\text{CC}_6\text{H}_5\text{F})+\text{Cu}^+]^+$. ^1H NMR (300 MHz, CDCl_3): 6.90~7.40 (m, 12 H, $-\text{C}_8\text{H}_4\text{F}$), 5.04~4.82 (m, 12 H, CH), 4.76 (bs, 2H, $\mu_4\text{-H}$), 1.21~1.88 (d, 72 H, CH_3) ppm; ^{13}C NMR (400 MHz, $d\text{-Acetone}$): 159.63, 133.42, 116.68, 81.57, 74.23, 74.07, 72.92, 54.75, 23.31 ppm; ^{31}P NMR (121.49 MHz, CDCl_3): 103.6. (**2_H**). FT-IR data in KBr pellet (cm^{-1}): 3063.8; 2977.3; 2932.4; 2871.9; 2001.6; 1601.5 1574.6; 1465.71257.5; 1238.8; 1177.0; 1103.1; 1075.4; 884.3; 746.0; 680.1; 529.1 460.2. Elem. Anal: (Cal. C% 30.82; H% 4.23). Found: C% 27.25; H% 4.46. The percentage yield: 0.030 g, 47.3 % based on Cu.

(2_D): ESI-MS: m/z (Cal. 2337.43) 2338.52 for $[\text{Cu}_{11}(\text{D})_2\{\text{S}_2\text{P}(\text{O}^i\text{Pr})_2\}_6(\text{C}\equiv\text{CC}_6\text{H}_5\text{F})_3]$ (**2_D**) and m/z (Cal. 2400.36) 2402.53 for $[\text{Cu}_{11}(\text{D})_2\{\text{S}_2\text{P}(\text{O}^i\text{Pr})_2\}_6(\text{C}\equiv\text{CC}_6\text{H}_5\text{F})_3]+\text{Cu}^+]^+$. ^1H NMR (300 MHz, CDCl_3): 6.91~7.39 (m, 12 H, $-\text{C}_2\text{Ph}$), 5.03~4.82 (m, 12 H, CH), 1.24~1.39 (d, 72 H, CH_3) ppm. ^2H NMR (46.1 MHz, CDCl_3): 4.82 (bs, 2D, $\mu_4\text{-D}$). ^{31}P NMR (121.49 MHz, CDCl_3): 103.6. (**2_D**). FT-IR data in KBr pellet (cm^{-1}): 3436.2; 3064.9; 2977.5; 2932.6; 2872.7; 2000.4; 1602.9; 1574.8; 1480.8; 1450.7 1257.6; 1258.6; 1177.7; 1102.5; 1075.0; 934.0; 884.9; 754.9; 680.8; 529.5; 460.0. The percentage yield: 0.035 g, 55.3% based on Cu.

(3_H): ESI-MS: m/z (Cal. 2373.49) 2373.48 for $[\text{Cu}_{11}(\text{H})_2\{\text{S}_2\text{P}(\text{O}^i\text{Pr})_2\}_6(\text{C}\equiv\text{CC}_6\text{H}_4\text{OCH}_3)_3]$ (**3_H**) and m/z (Cal. 2436.42) 2436.41 for $[\text{Cu}_{11}(\text{D})_2\{\text{S}_2\text{P}(\text{O}^i\text{Pr})_2\}_6(\text{C}\equiv\text{CC}_6\text{H}_4\text{OCH}_3)_3]+\text{Cu}^+]^+$. ^1H NMR (300 MHz, CDCl_3): 6.70~7.26 (m, 15 H, $-\text{C}_9\text{H}_7\text{O}$), 5.03~4.80 (m, 12 H, CH), 4.65 (bs, 2H, $\mu_4\text{-H}$), 3.78 (s, 3H- $\text{CH}_3\text{C}_8\text{H}_4\text{O}$) 1.21~1.88 (d, 72 H, CH_3) ppm; ^{13}C NMR (400 MHz, $d\text{-Acetone}$): 159.63, 133.42, 116.36, 113.68, 81.57, 74.29, 74.07, 72.92, 54.79, 23.31 ppm; ^{31}P NMR (121.49 MHz, CDCl_3): 104.0. (**3_H**). FT-IR data in KBr pellet (cm^{-1}): 3068.4; 2974.6; 2931.2; 2872.1;

2000.9; 1601.7; 1503.9; 1259.9; 1177.1; 1025.1; 829.9; 756.7; 637.1; 532.1; 488.2. Elem.Anal: (Cal. C% 31.87; H% 4.54). Found: C% 31.82; H% 4.54. The presentage yield is 20.4% based on Cu.

(3D): ESI-MS: m/z (Cal.2373.49) 2375.49 for $[\text{Cu}_{11}(\text{D})_2\{\text{S}_2\text{P}(\text{O}^i\text{Pr})_2\}_6(\text{C}\equiv\text{CC}_6\text{H}_4\text{OCH}_3)_3]$ (**3D**) and m/z (Cal. 2436.42) 2438.42 for $[\text{Cu}_{11}(\text{D})_2\{\text{S}_2\text{P}(\text{O}^i\text{Pr})_2\}_6(\text{C}\equiv\text{CC}_6\text{H}_4\text{OCH}_3)_3+\text{Cu}^+]^+$. ^1H NMR (300 MHz, CDCl_3): ^1H NMR (300 MHz, CDCl_3): (m, 15 H, $-\text{C}_9\text{H}_7\text{O}$), (m, 12 H, CH), (bs, 2H, $\mu_4\text{-H}$), (s, 3H- $\text{CH}_3\text{C}_8\text{H}_4\text{O}$) (d, 72 H, CH_3) ppm ppm. ^2H NMR (46.1 MHz, CDCl_3): (bs, 2D, $\mu_4\text{-D}$). ^{31}P NMR (121.49 MHz, CDCl_3): 104.0. (**3D**). FT-IR data in KBr pellet (cm^{-1}): 3033.9; 2974.7; 2931.2; 2871.8; 2001.9, 1601.6; 1503.9; 1251.9; 1169.8; 1026.4; 820.1; 748.3; 636.2; 531.2; 457.7. The presentage yield: 19.7% based on Cu.

Single Crystal X-ray Crystallography

Single crystals suitable for X-ray diffraction analysis of **1**, **2** and **3** were obtained by slowly diffusing hexane into a concentrated acetone solution at $-5\text{ }^\circ\text{C}$ temperature. During the crystallization of **1** in acetone solution, the cocrystal of **1** and $[\text{Cu}_7\text{H}]$ also grow at the same time. The single crystals were mounted on the tip of glass fiber coated in paratone oil, then frozen at 150 K. Data were collected on a Bruker APEX II CCD diffractometer using graphite monochromated Mo $\text{K}\alpha$ radiation ($\lambda = 0.71073\text{ \AA}$). Absorption corrections for area detector were performed with SADABS¹⁷ and the integration of raw data frame was performed with SAINT¹⁸. The structure was solved by direct methods and refined by least-squares against F^2 using the SHELXL-2018/3 package,¹⁹⁻²⁰ incorporated in SHELXTL/PC V6.14.²¹ All non-hydrogen atoms were refined anisotropically. Hydride atoms were located from the residual electron densities and refined without any constraints. In structure of **1**, carbon atoms on O10, O12, and phenyl ring on C54 were disordered and split into two positions with 50% occupancy at each. The solvent molecules were severe disordered. SQUEEZE²² program is applied to remove the peaks of unmodelled solvent molecules. In structure of **2**, three $[\text{Cu}_{11}(\text{H})_2\{\text{S}_2\text{P}(\text{O}^i\text{Pr})_2\}_6(\text{C}\equiv\text{CC}_6\text{H}_4\text{F})_3]$ molecules were solved in asymmetric unit. One of three Cu_{11} clusters has minor contribution of $[\text{Cu}_{11}(\text{S})\{\text{S}_2\text{P}(\text{O}^i\text{Pr})_2\}_6(\text{C}\equiv\text{CC}_6\text{H}_4\text{F})_3]$. The occupancy ratio of S^{2-} and two H is 20:80. The other two Cu_{11} molecules in asymmetric unit did not reveal heavy electron densities in the center of Cu_{11} framework. One phenyl ring on C98 was found to be disordered, and split into three

positions. The structure reported herein has been deposited at the Cambridge Crystallographic Data Centre, CCDC 1961353 (1), CCDC 1961354 (2), and CCDC 1961355 (3).

Single Crystal Neutron Diffraction

The location of hydrides in $\mathbf{1}_N$ was confirmed by single crystal neutron diffraction experiment using the TOPAZ single-crystal neutron time-of-flight (TOF) Laue diffractometer at ORNL's Spallation Neutron Source.²³ A light yellow plate-shaped crystal (1.75×1.24×0.8 mm) was attached to a MiTeGen loop using a perfluorinated grease (Krytox GPL 205) and cooled to 100 K for data collection. A total of 20 crystal orientations optimized with CrystalPlan software²⁴ were used to ensure better than 98% coverage of a hemisphere of reciprocal space. Each orientation was measured for approximately 4 hrs. Raw peaks intensities were obtained using the 3-D ellipsoidal Q-space integration method available in Mantid.²³ Data normalization including Lorentz, neutron δ TOF spectrum, and detector efficiency corrections were carried out with the ANVRED3 program.²⁵ A Gaussian numerical absorption correction was applied with $\mu = 1.1587 + 0.8921 \lambda \text{ cm}^{-1}$. The reduced data were saved in SHELX HKLF2 format in which the neutron wavelength for each reflection was recorded separately. Non-hydrogen atom positions in the X-ray structure were used for initial refinement of the neutron structure. Hydrogen atoms on carbon atoms are placed using the riding model available in SHELXL-2014²⁶ with the default C-H distances for neutrons; only their displacement parameters are refined. The hydride in the asymmetric unit of $\mathbf{1}_N$ was located from the difference Fourier map calculated using the neutron data. Hydrogen is a negative scatter for neutrons. The deepest and the second deepest hole of -3.36 and -2.64 fm \AA^{-3} located $\sim 1.68 \text{ \AA}$ from the Cu5 and Cu3 atom, respectively, were assigned as the two hydride atoms in Cu₁₁ cluster. The third deepest hole of -2.17 fm \AA^{-3} located $\sim 1.57 \text{ \AA}$ from Cu12 was assigned as the hydride atom in Cu₇ cluster. The neutron structure was then refined successfully to convergence using the SHELXL-2014 program. Crystal data and selected distances are listed in Tables 1-2. The structure reported herein has been deposited at the Cambridge Crystallographic Data Centre, CCDC 1967640 (2[$\mathbf{1}_N$][$\mathbf{4}_N$] . 2[(CH₃)₂CO]).

Computational details

Geometry optimizations were performed by DFT calculations with the Gaussian 16 package,²⁷ using the PBE0 functional,²⁸ together with Grimme's empirical DFT-D3 corrections²⁹ and the all-electron Def2-TZVP set from EMSL Basis Set Exchange Library.³⁰ All the optimized geometries were characterized as true minima on their potential energy surface by harmonic vibrational analysis. The Wiberg bond indices were computed with the NBO 6.0 program.³¹ The ¹H NMR chemical shift were computed, according to the GIAO method,³² as implemented in Gaussian 16. The UV–visible transitions were calculated by means of TD-DFT calculations. Only singlet-singlet, *i.e.* spin-allowed, transitions were computed. The UV–visible spectra were simulated from the computed from TD-DFT³³ transitions and their oscillator strengths by using the SWizard program,³⁴ each transition being associated with a Gaussian function of half-height width equal to 3000 cm⁻¹. The compositions of the molecular orbitals were calculated using the AOMix program.³⁵

ASSOCIATED CONTENT

The Supporting Information is available free of charge on the ACS Publications website at DOI:

AUTHOR INFORMATION

Corresponding Author

* E-mail: chenwei@mail.ndhu.edu.tw. Tel: +886-3-8903607. Fax: +886-3-8903570.

Notes

The authors declare no competing financial interest.

ACKNOWLEDGMENTS

This work was supported by the Ministry of Science and Technology of Taiwan (MOST 106-2113-M-259-010, 108-2923-M-259-001), the France-Taiwan ANR-MOST 2018 program (project Nanoalloys) and the GENCI French national computer resource center (grant

A0030807367). Single crystal neutron diffraction performed on TOPAZ used resources at the Spallation Neutron Source, a DOE Office of Science User Facility operated by the Oak Ridge National Laboratory, under Contract No. DE-AC05-00OR22725 with UT-Battelle, LLC.

REFERENCES

- 1) (a) Shima, T.; Luo, Y.; Stewart, T.; Bau, R.; McIntyre, G. J.; Mason, S. A.; Hou, Z. Molecular heterometallic hydride clusters composed of rare-earth and d-transition metals. *Nat. Chem.* **2011**, *3*, 814-820 (b) Dhayal, R. S.; Liao, J.-H.; Kahlal, S.; Wang, X.; Liu, Y.-C.; Chiang, M.-H.; van Zyl, W. E.; Saillard, J.-Y.; Liu, C. W. [Cu₃₂(H)₂₀{S₂P(OⁱPr)₂}₁₂]: The Largest Number of Hydrides Recorded in A Molecular Nanocluster by Neutron Diffraction. *Chem. Eur. J.* **2015**, *21*, 8369-8374. (c) Dhayal, R. S.; Liao, J.-H.; Wang, X.; Liu, Y.-C.; Chiang, M.-H.; Kahlal, S.; Saillard, J.-Y.; Liu, C. W. Diselenophosphate-Induced Conversion of an Achiral [Cu₂₀H₁₁{S₂P(OⁱPr)₂}₉] into a Chiral [Cu₂₀H₁₁{Se₂P(OⁱPr)₂}₉] Polyhydrido Nanocluster. *Angew. Chem. Int. Ed.* **2015**, *54*, 13604-13608. (d) Edwards, A. J.; Dhayal, R. S.; Liao, P.-K.; Liao, J.-H.; Chiang, M.-H.; Piltz, R. O.; Kahlal, S.; Saillard, J.-Y.; Liu, C. W. Chinese puzzle molecule; a 15 hydride, 28 copper atom nanoball. *Angew. Chem. Int. Ed.* **2014**, *53*, 7214-7218. (e) Dhayal, R. S.; Liao, J.-H.; Lin, Y.-R.; Liao, P.-K.; Kahlal, S.; Saillard, J.-Y.; Liu, C. W. A nanospheric polyhydrido copper cluster of elongated triangular orthobicupola array; liberation of H₂ from solar energy. *J. Am. Chem. Soc.* **2013**, *135*, 4704-4707. (f) Liao, J.-H.; Dhayal, R. S.; Wang, X.; Kahlal, S.; Saillard, J.-Y.; Liu, C. W. Neutron diffraction studies of a four-coordinated hydride in near square-planar geometry. *Inorg. Chem.* **2014**, *53*, 11140-11145.
- 2) (a) Haiduc, I. Inverse coordination - An emerging new chemical concept. Oxygen and other chalcogens as coordination centers. *Coord. Chem. Rev.* **2017**, *338*, 1-26, and references cited there in. (b) Haiduc, I. Inverse coordination – An emerging new chemical concept. II. Halogens as coordination centers. *Coord. Chem. Rev.* **2017**, *348*, 71-91, and references cited there in.
- 3) (a) Liu, C. W.; Stubbs, R. T.; Staples, R. J.; Fackler J. P., Jr. Syntheses and Structural Characterization of Two New Cu-S Cluster of Dialkyl Dithiophosphate: A Sulfide-Centered Cu₈ Cube, {Cu₈[S₂P(OⁱPr)₂]₆(μ₈-S)}, and a Distorted Octahedral

- {Cu₆[S₂P(OEt)₂]₆.2H₂O} Cluster. *J. Am. Chem. Soc.* **1995**, *117*, 9778-9779. (b) Fackler, J. P., Jr.; Staples, R. J.; Liu, C. W.; Stubbs, R. T.; Lopez, C.; Pitts, J. T. Octahedral, Cubal and centered Cubal Dithiolate Clusters and Cages of Cu(I) and Ag(I). *Pure Appl. Chem.* **1998**, *70*, 839-844. (c) Fackler, J. P., Jr. Forty-Five Years of Chemical Discovery Including a Golden Quarter-Century. *Inorg. Chem.* **2002**, *41*, 6959-6972. (d) Huang, Z.-X.; Lu, S.-F.; Huang, J.-Q.; Wu, D.-M.; Huang, J.-L. Synthesis and structure of Cu₈S[S₂P(OC₂H₅)₂]₆. *J. Struct. Chem.* **1991**, *10*, 213-217. (e) Wu, D.-M.; Huang, J.-Q.; Lin, Y.; Haung, J.-L. Study on the reaction performance of cluster compound- a reaction of copper(+2) capturing ligands from molybdenum cluster and the crystal structure of its product Cu₈Cl[S₂P(OEt)₂]₆. *Sci. Sin. Ser. B (Engl. Ed.)* **1988**, *31*, 800-806. (f) Matsumoto, K.; Tanaka, R.; Shimomura, R.; Nakao, Y. Synthesis and X-ray structures of octanuclear silver(I) cluster [Ag₈(μ₆-S){S₂P(OC₂H₅)₂]₆] and its copper(I) analogue [Cu₈(μ₈-S){S₂P(OC₂H₅)₂]₆]. *Inorg. Chim. Acta* **2000**, *304*, 293-296. (g) Latouche, C.; Liu, C.-W.; Saillard, J.-Y. Encapsulating hydrides and main-group anions in d10-metal clusters stabilized by 1,1-dichalcogeno ligands. *J. Clust. Sci.* **2014**, *25*, 147-171.
- 4) Liu, C. W.; Chen, H.-C.; Wang, J.-C.; Keng, T.-C. First selenide-centered Cu₈ cubic cluster containing dialkyldiselenophosphate ligands. X-ray structures Cu₈(μ₈-Se)[Se₂P(OⁱPr)₂]. *Chem. Commun.* **1998**, 1831-1832.
- 5) Liu, C. W.; Shang, I.-J.; Wang, J.-C.; Keng, T.-J. Metal dialkyl diselenophosphate; a rare example of co-crystallization with clusters, Ag₈(μ₈-Se)[Se₂P(OⁱPr)₂]₆ and Ag₆[Se₂P(OⁱPr)₂]₆. *Chem. Commun.* **1999**, 995-996.
- 6) (a) Liu, C. W.; Hung, C.-M.; Santra, B. K.; Chen, H.-C.; Hsueh, H.-H.; Wang, J.-C. Novel chloride-centered discrete Cu₈^I cubic cluster containing diselenophosphate ligands. Syntheses and structures of Cu₈(μ₈-Cl)[Se₂P(OR)₂]₆PF₆ (R = Et, Pr, ⁱPr). *Inorg. Chem.* **2003**, *42*, 3216-3220.; (b) Liu, C. W.; Hung, C.-M.; Chen, H.-C.; Wang, J.-C.; Keng, T.-C.; Guo, K.-M. A novel nanocoordinate bridging selenido ligand in a tricapped trigonal prismatic geometry. X-ray structure of Cu₁₁(μ₉-Se)(μ₃-Br)[Se₂P(OⁱPr)₂]₆. *Chem. Commun.* **2000**, 1897-1998.
- 7) (a) Liu, C. W.; Haia, H.-C.; Hung, C.-M.; Santra, B. K.; Liaw, B.-J.; Wang, J.-C.; Lin, Z. New halide-centered discrete Ag₈^I cubic cluster containing diselenophosphate ligands, Cu₈(μ₈-X)[Se₂P(OR)₂]₆PF₆ (X = Cl, Br; R = Et, Pr, ⁱPr). *Inorg. Chem.* **2004**, *43*, 4464-

- 4470.; (b) Liu, C. W.; Hung, C.-M.; Haia, H.-C.; Liaw, B.-J.; Liou, L.-S.; Tsai, Y.-F.; Wang, J.-C. $\text{Ag}_8\text{Cl}_2[\text{Se}_2\text{P}(\text{OEt})_2]_6$: A Rare Example Containing a Combination of Discrete Clusters and Chains. *Chem. Commun.* **2003**, 976-977.
- 8) (a) Liu, C. W.; Hung, C.-M.; Wang, J.-C.; Keng, T.-C. Characterizations of $\text{Cu}_{11}(\mu_9\text{-Se})(\mu_3\text{-I})[\text{Se}_2\text{P}(\text{OR})_2]_6$ (R = iPr, Pr) by X-ray diffraction and multinuclear NMR. *J. Chem. Soc., Dalton Trans.* **2002**, 3482-3488. (b) Liu, C. W.; Hung, C.-M.; Santra, B. K.; Chu, Y.-H.; Wang, J.-C.; Lin, Z. A Nanocoordinated Bridging Selenide in a Tricapped Trigonal Prismatic Geometry Identified Copper Cluster in Undecanuclear Cluster. Syntheses, Structures and DFT calculation. *Inorg. Chem.* **2004**, *43*, 4306-4316. (c) Hung, C.-M.; Chu, Y.-H.; Santra, B. K.; Liaw, B.-J.; Wang, J.-C.; Liu, C. W. J. Intermolecular Se Interactions Identified in $\text{Cu}_{11}(\mu_9\text{-Se})(\mu_3\text{-I})[\text{Se}_2\text{P}(\text{OEt})_2]_6$ form a one dimensional polymeric chain. *J. Chin. Chem. Soc.* **2006**, *53*, 825-830.
- 9) (a) Liu, C. W.; Feng, C.-S.; Fu, R.-J.; Chang, H.-W.; Saillard, J.-Y.; Kahlal, S.; Wang, J.-C.; Chang, I.-J. Structure, Photophysical Properties, and DFT Calculations of Selenide-Centered Pentacapped Trigonal Prismatic Silver(I) cluster. *Inorg. Chem.* **2010**, *49*, 4934-4941. (b) Liu, C. W.; Shang, I. J.; Fu, R.-J.; Liaw, B.-J.; Wang, J.-C.; Chang, I.-J. Selenium-Centered Undecanuclear Silver Cages Surrounded by Iodo and Dialkyl Diselenophosphato Ligands; Syntheses, Structures, and Photophysical Properties. *Inorg. Chem.* **2006**, *45*, 2335-2340.
- 10) Li, Y.-J.; Latouche, C.; Kahlal, S.; Liao, J.-H.; Dhayal, R. S.; Saillard, J.-Y.; Liu, C.W. A μ_9 -Iodide in a Tricapped Trigonal-Prismatic Geometry. *Inorg. Chem.* **2012**, *51*, 7439-7441.
- 11) Li, B.; Liao, J.-H.; Tang, H.-T.; Li, Y.-J.; Liu, C. W. Substitution reactions on a hypercoordinated main-group element encapsulated in a pentacapped trigonal prismatic copper cage. *Dalton Trans.* **2013**, *42*, 14384-14387.
- 12) Chakrahari, K. K.; Liao, J.-H.; Kahlal, S.; Liu, Y.-C.; Chiang, M.-H.; Saillard, J.-Y.; Liu, C. W. $[\text{Cu}_{13}(\text{S}_2\text{CN}^n\text{Bu})_6(\text{acetylide})_4]^+$: A Two-Electron Superatom. *Angew. Chem. Int. Ed.* **2016**, *55*, 14.
- 13) Liao, P.-K.; Fang, C.-S.; Edwards, A. J.; Kahlal, S.; Saillard, J.-Y.; Liu, C. W. Hydrido copper cluster supported by dithiocarbamates: oxidative hydride removal and neutron diffraction analysis of $[\text{Cu}_7(\text{H})\{\text{S}_2\text{C}(\text{aza-15-crown-5})\}_5]$. *Inorg. Chem.* **2012**, *51*, 6577-6591.

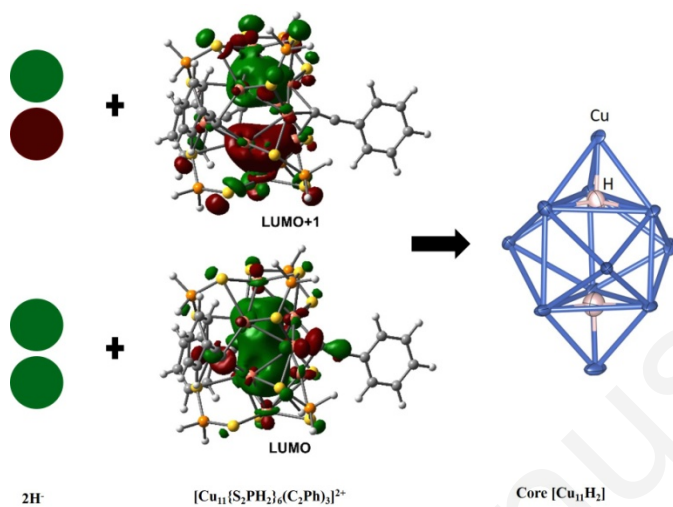
- 14) a) Dhayal, R. S.; van Zyl, W. E.; Liu, C. W. Polyhydrido Copper Clusters: Synthesis Advances, Structural Diversity, and Nanocluster-to-Nanoparticle Conversion. *Acc. Chem. Res.* **2016**, *49*, 86-95. b) Dhayal, R. S.; van Zyl, W. E.; Liu, C. W. Copper hydride clusters in energy storage and conversion. *Dalton Trans.* **2019**, *48*, 3531-3548. c) Sun, C.; Mammen, N.; Kaappa, S.; Yuan, P.; Deng, G.; Zhao, C.; Yan, J.; Malola, S.; Honkala, K.; Häkkinen, H.; Teo, B. K.; Zheng, N. Atomically Precise, Thiolated Copper-Hydride Nanocluster as Single-Site Hydrogenation Catalysis for Ketones in Mild Conditions. *ACS Nano.*, **2019**, *13*, 5975-5986. d) Nguyen, T. A. D.; Jones, Z. R.; Goldsmith, B. R.; Buratto, W. R.; Wu, G.; Scott, S. L.; Hayton, T. W. A Cu₂₅ Nanocluster with Partial Cu(0) Character. *J. Am. Chem. Soc.*, **2015**, *134*, 13319-13324. e) Huertos, M. A.; Cano, I.; Bandeira, N. A. G.; Benet-Buchholz, J.; Bo, C.; van Leeuwe, P. W. N. M. Phosphinothiolates as Ligands for Polyhydrido Copper Nanocluster. *Chem. Eur. J.*, **2014**, *20*, 16121-16127. f) Li, J.; Ma, H. Z.; Reid, G. E.; Edwards, A. J.; Hong, Y.; White, J. M.; Mulder, R. J.; O'Hair, R. A. J. Synthesis and X-Ray crystallographic Characterization of Frustum-Shaped Ligated [Cu₁₈H₁₆(DPPE)₆]²⁺ and [Cu₁₆H₁₄(DPPA)₆]²⁺ Nanoclusters and Studies on Their H₂ Evolution Reactions. *Chem. Eur. J.* **2018**, *24*, 2070-2074. g) Nakamae, K.; Nakaima, T.; Ura, Y.; Kitagawa, Y.; Tanase, T. Facially Dispersed Polyhydride Cu₉ and Cu₁₉ Clusters Comprising Apex-Truncated Supertetrahedral and Square-face-Capped Cuboctahedral Copper Frameworks. *Angew. Chem. Int. Ed.*, **2019**, DOI: 10.1021/anie.201913533. h) Ghosh, A.; Huang, R.-W.; Alamer, B.; Abou-Hamad, E.; Hedhili, M. N.; Mohammed, O. F.; Bakr, O. M. [Cu₆₁(S^tBu)₂₆S₆C₁₆H₁₄]⁺: A Core-Shell Superatom Nanocluster with a Quasi-J₃₆ Cu₁₉ Core and an "18-Crown-6" Metal-Sulfide-like Stabilizing Belt. *ACS Materials Lett.*, **2019**, *1*, 297-302. i) Yuan, P.; Chen, R.; Zhang, X.; Chen, F.; Yan, J.; Sun, C.; Ou, D.; Peng, J.; Lin, S.; Tang, Z.; Teo, B. K.; Zheng, L.-S.; Zheng, N. Ether-Soluble Cu₅₃ Nanocluster as an Effective Precursor of High-Quality CuI Films for Optoelectronic Applications. *Angew. Chem. Int. Ed.*, **2018**, *58*, 835-839. j) Chen, A.; Kang, X.; Jin, S.; Du, W.; Wang, S.; Zhu, M. Gram-Scale Preparation of Stable Hydride M@Cu₂₄ (M=Au/Cu) Nanoclusters. *J. Phys. Chem. Lett.*, **2019**, *10*, 6124-6128.
- 15) Kubas, G. J.; Monzyk, B.; Crumbliss, A. L. Tetrakis(Acetonitrile)Copper(I) Hexfluorophosphate. *Inorg. Synth.* **1979**, *19*, 90-92.

- 16) Wystrach, P.; Hook, E. O.; Christopher, G. L. M. Notes – Basic Zinc Double Salt of O, O-Diakyl Phosphorodithio Acid. *J. Org. Chem.* **1956**, *21*, 705-707.
- 17) *SADABS*, version 2014-11.0, Bruker Area Detector Absorption Corrections (Bruker AXS Inc., Madison, WI, 2014).
- 18) *SAINT*, included in G. Jogl, V4.043: Software for the CCD detector system (Bruker Analytical: Madison, WI, 1995).
- 19) Sheldrick, G. M. *Acta Cryst. A* **2008**, *64*, 112-122.
- 20) Gruene, T.; Hahn, H. W.; Luebben, A. V.; Meilleur, F.; Sheldrick, G. M. *J. Appl. Cryst.* **2014**, *47*, 462-466.
- 21) *SHELXTL*, version 6.14. (Bruker AXS Inc., Madison, Wisconsin, USA, 2003).
- 22) *PLATON/SQUEEZE* Spek, A. L. *Acta Cryst.* **2009**, *D65*, 148-155.
- 23) Schultz, A. J.; Jorgensen, M. R. V.; Wang, X.; Mikkelsen, R. L.; Mikkelsen, D. J.; Lynch, V. E.; Peterson, P. F.; Green, M. L.; Hoffmann, C. M. *J. Appl. Cryst.* **2014**, *47*, 915-921.
- 24) Zikovsky, J.; Peterson, P. F.; Wang, X. P.; Frost, M.; Hoffmann, C. *J. Appl. Cryst.* **2011**, *44*, 418-423.
- 25) Schultz, A. J.; Srinivasan, K.; Teller, R. G.; Williams, J. M.; Lukehart, C. M. *J. Am. Chem. Soc.* **1984**, *106*, 999-1003.
- 26) Sheldrick, G. M. *Acta Cryst.* **2015**, *C71*, 3-8.
- 27) Gaussian 16, Revision C.01, Frisch, M. J.; Trucks, G. W.; Schlegel, H. B.; Scuseria, G. E.; Robb, M. A.; Cheeseman, J. R.; Scalmani, G.; Barone, V.; Petersson, G. A.; Nakatsuji, H.; Li, X.; Caricato, M.; Marenich, A. V.; Bloino, J.; Janesko, B. G.; Gomperts, R.; Mennucci, B.; Hratchian, H. P.; Ortiz, J. V.; Izmaylov, A. F.; Sonnenberg, J. L.; Williams-Young, D.; Ding, F.; Lipparini, F.; Egidi, F.; Goings, J.; Peng, B.; Petrone, A.; Henderson, T.; Ranasinghe, D.; Zakrzewski, V. G.; Gao, J.; Rega, N.; Zheng, G.; Liang, W.; Hada, M.; Ehara, M.; Toyota, K.; Fukuda, R.; Hasegawa, J.; Ishida, M.; Nakajima, T.; Honda, Y.; Kitao, O.; Nakai, H.; Vreven, T.; Throssell, K.; Montgomery, J. A., Jr.; Peralta, J. E.; Ogliaro, F.; Bearpark, M. J.; Heyd, J. J.; Brothers, E. N.; Kudin, K. N.; Staroverov, V. N.; Keith, T. A.; Kobayashi, R.; Normand, J.; Raghavachari, K.; Rendell, A. P.; Burant, J. C.; Iyengar, S. S.; Tomasi, J.; Cossi, M.; Millam, J. M.; Klene, M.; Adamo, C.; Cammi, R.; Ochterski, J. W.; Martin, R. L.; Morokuma, K.; Farkas, O.; Foresman, J. B.; Fox, D. J. Gaussian, Inc., Wallingford CT,

2016.

- 28) C. Adamo, A.; Barone, V. Toward reliable density functional methods without adjustable parameters: The PBE0 model. *J. Chem. Phys.* **1999**, *110*, 6158-69.
- 29) Grimme, S.; Ehrlich, S.; Goerigk, L. Effect of the damping function in dispersion corrected density functional theory. *J. Comp. Chem.* **2011**, *32*, 1456-65.
- 30) F. Weigend, F.; Ahlrichs, R. Balanced basis sets of split valence, triple zeta valence and quadruple zeta valence quality for H to Rn: Design and assessment of accuracy. *Phys. Chem. Chem. Phys.* **2005**, *7*, 3297-305.
- 31) Glendening, E.D.; Badenhop, J. K.; Reed, A. E.; Carpenter, J. E.; Bohmann, J. A.; Morales, C. M.; Landis, C. R.; Weinhold, F. NBO 6.0; Theoretical Chemistry Institute, University of Wisconsin, Madison, WI, 2013, <http://nbo6.chem.wisc.edu>.
- 32) Wolinski, K.; Hilton, J. F.; Pulay, P. Efficient Implementation of the Gauge-Independent Atomic Orbital Method for NMR Chemical Shift Calculations. *J. Am. Chem. Soc.* **1990**, *112*, 8251-60.
- 33) Ullrich, C. Time-Dependent Density-Functional Theory, Concepts and Applications, Oxford University Press, New York, **2012**.
- 34) Gorelsky, S. I. SWizard program, revision 4.5, <http://www.sg-chem.net>.
- 35) Gorelsky, S. I. AOMix program, <http://www.sg-chem.net>.

Image for Table of Contents



Accepted manuscript